IMPACT OF DISTRIBUTED GENERATIONS WITH EXTENDED-PLUG-IN HYBRID ELECTRIC VEHICLES

Abstract

The use of Distributed Generations (DGs) with Extended Plug-in Hybrid Electric Vehicles (Ex-PHEVs) will grow dramatically in the coming years. The relation to the distribution system of DGs with Ex-PHEV will contribute to future challenges. This chapter addresses the multi-tasking Genetic Algorithm optimization of DGs with Ex-PHEV planning in distribution systems for load models for rating and placement determination. From a system viewpoint, this research focuses on reducing total active power loss. The numerous DG kinds are considered from the investigation's point of view. Various kinds of constant impedance (Z), constant current (I), constant power (P) load models for Light-emitting diode, Laptop charger, Personal computer, Tungsten light, and Vacuum tube are taken into account while making DG plans to improve system performance indices. System performance indices are measured in this chapter in the same way as the active power loss index (% ILP), the reactive power loss index (% ILQ), the voltage deviation index (% IVD), the short circuit current reduction (% IC), the active power DG penetration (% $p_{\text{PWDG \& Ex-PHEV}}$) and the reactive power DG penetration (% $p_{\text{QWDG \& Ex-PHEV}}$). The viability of the aforementioned technique was confirmed on the 37-bus test distribution system.

Keywords: Distributed Generations, Distribution Systems, Extended Plug-in Hybrid Electric Vehicles, Performance Indices, Genetic Algorithm, ZIP Load Models.

Authors

Dilip Kumar Patel
Kamla Nehru Institute of Technology
Sultanpur, Uttar Pradesh, India.
dilippatelrec@gmail.com,

Deependra Singh
Kamla Nehru Institute of Technology
Sultanpur, Uttar Pradesh, India.
deependra_knit@yahoo.com,

Bindeshwar Singh
Kamla Nehru Institute of Technology
Sultanpur, Uttar Pradesh, India.
bindeshwar.singh2025@gmail.com

Abbreviations

DGs	Distributed Generations
EVs	Electric Vehicles
Ex-PHEV	Extended-Plug-in Hybrid Electric Vehicles
LMs	Load models
MVA	Mega Volt Ampere
ZIP - LMs	Constant impedance (Z), Constant current (I), Constant power (P) loads models

Symbols

p_g, and q_g	Active and reactive power delivered by the main substation
p_{dg1}, p_{dg2}, and p_{dg4}	Active power delivered by DG1, DG2, and DG4 accordingly
q_{dg2} , and q_{dg3}	Reactive power delivered by DG2 and DG3 accordingly
q_{dg4}	Reactive power delivered/consumed by DG4
$s_{\mathrm{DG}} - l_{DG}$	Size-location pair of DGs
$s_{Ex-PHEV} - l_{Ex-PHEV}$	Size-location pair of Ex-PHEV
$p_{WEx-PHEV}$	Active power delivered by Ex-PHEV
$p_{WODG\&Ex-PHEV}$	Active power without DGs and Ex-PHEV
$q_{WEx-PHEV}$	Reactive power delivered by Ex-PHEV
$q_{WODG\&Ex-PHEV}$	Reactive power without DGs and Ex-PHEV
$p_{PWDG\&Ex-PHEV}$	Active power penetration of DGs and Ex-PHEV
$p_{QWDG\&Ex-PHEV}$	Reactive power penetration of DGs and Ex-PHEV

I. INTRODUCTION

Plug-in hybrid electric vehicles (PHEVs) have become more and more widespread in the past few years thanks to their environmental benefits over standard vehicles. In the upcoming years, PHEV usage on smart grids is anticipated to increase. There will be new issues once PHEVs are connected to the distribution network.

Galiveeti et al. [1] presented the Impact of PHEV and DG on the dependability of distribution systems for enhancement of penetration. Pazouki et al. [2] discussed the simultaneous planning of plug-in electric vehicles (PEVs) charging stations and DGs considering financial, technical, and environmental effects. Over the next few decades, the use of PEVs and DG is expected to rise. If both innovations were to be widely and unrestrainedly exploited, the electric grid might suffer. The negative consequences of each of these technologies, however, might be reduced with the proper fusion of them and the addition of some storage. Developing grid-connected systems with PEV chargers, DG, and storage requires a framework and methodology, which is precisely outlined in [3]. Taking into consideration the uncertainty concerning wind speed variations and PEV charging, Monte Carlo simulation is used to examine the interaction among wind-based DG and PEVs in [4]. Vehicle-to-grid (V2G) systems are growing in popularity and may eventually rule the motor vehicle sector. For charging and discharging operations, the V2G batteries include corporate parking lots. The time correlation between EV charging and photovoltaic (PV), if it is proposed to use PV to charge the EVs, is addressed in [5]. Integrated energy monitoring of PEVs in a power grid with renewable for minimizing the overall operating cost and offering frequency control discussed in ref. [6]. A two-stage comprehensive DG investment strategy framework that may manage EV charging needs and volatility in renewable energy is discussed in [7]. For DGs, a multi-objective planning model was proposed that takes into account transportation loads as well as traditional source-load spatiotemporal scenarios presented in [8]. To address the issues originating from PEV instability, Ali et al. [9] address the problems brought on the PEV instability. PEVs with dispersed renewable energy sources can delay power system expenditures, lower well-to-wheels greenhouse gas emissions, and encourage the usage of renewable energy. Zhang et al. [10] proposed an accelerated generalized benders decomposition-based joint PEV charging network and distributed PV generation planning. In [11] a transactive real-time EV charging management method for commercial structures having PV on-site generation and service for EV charging is proposed for the building energy monitoring system. Wang et al. [12] suggested a distribution system extension planning framework which considers a variety of energy options on the distribution side, such as sharing EV charging stations, solar-based DG resources, and energy storage batteries. Ganguly et al. [13] proposed an adaptive genetic algorithm (GA) to develop a DG allocation strategy for radial distribution networks with load and generation uncertainties. For certain issues, an optimization method called a multi-objective GA is utilized. GA has currently been recognized as being especially well suited to multi-objective optimization problems, as it can create a whole range of multi-objective techniques at the same time. As a result, the optimization algorithms [14] - [15] are operating in this manner. For DGs and EVs planning with load models in distribution systems for improving system performance, the coefficient of ZIP-LMs is addressed in [16] - [17]. To improve system performances, Patel et al. [18] discussed a suggested technique called the GA-based technique for various kinds of DGs in the distribution system. To investigate the energy-saving potential of PHEVs, a predictive energy management technique using travel route data is described in [19]. Fuel

cell/battery hybrid electric vehicles can operate more effectively due to a system called energy management, which is discussed in [20].

Furthermore, Energy planners have to include DGs with Ex-PHEV units in the distribution system because they are easy to use, effective, and valuable for exploration and exploitation. As a result, the authors discovered that DGs with Ex-PHEV integration have all of the aforementioned characteristics.
A list of the chapter's major achievements is shown below:

- The research investigation revealed that system performance indices for providing various forms of DGs with Ex-PHEV for ZIP-LMs were analyzed throughout the chapter.
- The recommended GA technique is designed to improving the system performance indicators to decrease the entire active power loss while installing DGs with Ex-PHEV planning in distribution systems for ZIP-LMs.
- By boosting the system performance indicators, the suggested GA-OPF solution would handle severely constrained DG with Ex-PHEV allocating challenges and lower the overall active power loss.

The rest of the chapter is organized as outlined below: The Formulating Mathematical Issues is stated in the following part 2. Part 3 describes the execution of the GA. Part 4 describes multi-objective function-based formulations. The focus is on the outcomes and discussion in part 5. Finally, section 6 discusses the research conclusions and future directions of the paper.

II. FORMULATING MATHEMATICAL ISSUES

The integration of DGs with EV operation is crucial to distribution system planning. For the impact of DGs with Ex-PHEV planning, goal functions, and performance indices are presented in *sub-sections 2.1-2.3*, subsequently.

1. **DGs with Ex-PHEV Planning:** The DGs are classed as supporting actual and reactive power supplied or absorbed in general:
   - When the power factor is one, DG1 solely supplies the system with active power. Examples of DG1 include biogas, photovoltaic cells, and photovoltaic arrays.
   - DG2 provides the system with both active and reactive power at leading power factors of 0.80 to 0.99. Diesel, combustion engines, etc. are illustrations.
   - DG3 uses a power factor of 0.00 to provide the system with only reactive power. As an illustration, consider synchronous condensers, inductor banks, and capacitors.
   - Using lagging power factors of 0.80 to 0.99, depending on the operating situation, DG4 supplies active power to the system while absorbing or supplying reactive power. As an instance, doubly-fed induction generators powered by wind.

   In [21], the four-quadrant operation of DGs and their characteristics are discussed. A PHEV is a hybrid electric vehicle with two power sources. It has a rechargeable battery that can be charged by connecting it to a power source. PHEVs are more powerful than traditional electric vehicles because they have a higher battery storage capacity and are supported by fuel. Aside from that, electric vehicles are well known for significantly

reducing toxic gas emissions from gasoline combustion, such as carbon dioxide (CO2), which causes the greenhouse effect and global warming, carbon monoxide (CO), which occurs when incomplete combustion, hydrocarbons (CxHy), nitrogen oxides (NOx), and particulate matter (PM), also known as toxic smoke. Equation (1) indicates the total MVA input for the main substation without DGs and Ex-PHEV ($S_{WODG\&Ex-PHEV}$)

$$S_{WODG\&Ex-PHEV} = \sqrt{{p_g}^2 + {q_g}^2} \tag{1}$$

Equation (2) indicates the entire MVA input for the centralized substation without active power dg1 and Ex-PHEV ($S_{wodg1\&Ex-PHEV}$)

$$S_{wodg1\&Ex-PHEV} = \sqrt{(p_g + p_{dg1})^2 + {q_g}^2} \tag{2}$$

The whole MVA input for the centralized substation without active and reactive power dg2 and Ex-PHEV
($S_{wodg2\&Ex-PHEV}$) is shown in equation (3)

$$S_{wodg2\&Ex-PHEV} = \sqrt{(p_g + p_{dg2})^2 + \left(q_g + q_{dg2}\right)^2} \tag{3}$$

Equation (4) indicates the entire MVA input for the centralized substation without reactive power dg3 and Ex-PHEV ($S_{wodg3\&Ex-PHEV}$)

$$S_{wodg3\&Ex-PHEV} = \sqrt{{p_g}^2 + \left(q_g + q_{dg3}\right)^2} \tag{4}$$

Equation (5) indicates the entire MVA input for the centralized substation without active & reactive power dg4 and Ex-PHEV ($S_{wodg4\&Ex-PHEV}$)

$$S_{wodg4\&Ex-PHEV} = \sqrt{(p_g + p_{dg4})^2 + \left(q_g \pm q_{dg4}\right)^2} \tag{5}$$

Equation (6) indicates the entire MVA input for the centralized substation with active power dg1 and Ex-PHEV ($S_{wdg1\&Ex-PHEV}$)

$$S_{wdg1\&Ex-PHEV} = \sqrt{(p_g + p_{dg1} + p_{Ex-PHEV})^2 + (q_g + q_{Ex-PHEV})^2} \tag{6}$$

Equation (7) indicates the entire MVA input for the centralized substation with active & reactive power dg2 and Ex-PHEV ($S_{wdg2\&Ex-PHEV}$)

$$S_{wdg2\&Ex-PHEV} = \sqrt{(p_g + p_{dg2} + p_{Ex-PHEV})^2 + \left(q_G + q_{DG2} + q_{Ex-PHEV}\right)^2} \tag{7}$$

Equation (8) indicates the entire MVA input for the centralized substation with reactive power dg3 and Ex-PHEV ($S_{wdg3\&Ex-PHEV}$)

$$S_{wdg3\&Ex-PHEV} = \sqrt{(p_g + p_{Ex\_PHEV})^2 + \left(q_g + q_{dg3} + q_{Ex\_PHEV}\right)^2} \tag{8}$$

Equation (9) indicates the entire MVA input for the centralized substation with real and reactive power dg4 and Ex-PHEV ($S_{wdg4\ \&\ Ex-PHEV}$)

$$S_{wdg4\ \&\ Ex-PHEV} = \sqrt{(p_g + p_{dg4} + p_{Ex-PHEV})^2 + \left(q_g \pm q_{dg4} + q_{Ex-PHEV}\right)^2} \tag{9}$$

The ZIP model is a voltage-dependent mixed load model that includes constant impedance (Z), constant current (I), and constant power (P) loads with Z + I + P = 100%. The expression reflecting the active and reactive power for the ZIP load models [16] is presented in equs. (10) - (11).

$$p = p_0\left[Z_p\left(\frac{V_i}{V_0} + I_p\frac{V_i}{V_0} + p_p\right)\right] \tag{10}$$

$$q = q_0\left[Z_q\left(\frac{V_i}{V_0} + I_q\frac{V_i}{V_0} + p_q\right)\right] \tag{11}$$

Here p and q denotes the active and reactive powers at operating voltage (V_i); p_0 and q_0 denotes the active and reactive powers at rated voltage (V_0); Z_p, I_p and P_p denotes the ZIP - LMs coefficients for active power; Z_q, I_q and p_q denotes the ZIP - LMs coefficients of reactive power. In [16] the ZIP-LMs and their coefficients of real and reactive power are addressed.

2. **Goal Functions:** The goal function is the reduction of the system's overall active power loss (p_L). The expression of p_L is provided by equation (12).

$$p_L = \sum_{i,j\in N_L} \frac{p^2 + q^2}{|V_i|^2} r_{ij} \tag{12}$$

The p_L depends on the system bus voltage (V_i) and line resistances (r_{ij}). The restrictions on equality and inequality are as follows. The following are the equality limitations for DGs with Ex-PHEV planning:

The following are the equality restrictions of DGs using Ex-PHEV planning:

- The entire active power generation (p_{GT}) and DG units (p_{DGT}) necessary to meet the whole load demand (p_{DT}) and the entire active power loss (p_{LT}) are provided by equation (13).

$$p_{GT} + p_{DGT} - p_{DT} - p_{LT} = 0 \tag{13}$$

- The entire reactive power generated by traditional generation (q_{GT}) and DG units (q_{DGT}) must meet the total load demand (q_{DT}) and the total active power loss (q_{LT}) is calculated using equation (14).

$$q_{GT} + q_{DGT} - q_{DT} - q_{LT} = 0 \tag{14}$$

The following are the inequality limitations of DGs using Ex-PHEV planning:

- The bus voltage (V_m) at the bus I is limited by its lower and upper limitations ($V_m^{\min}$ and $V_m^{\max}$) and is determined by equation (15) for all buses.

$$V_m^{\min} \le V_m \le V_m^{\max}, \forall \mathrm{m} \in \{\text{number of buses}\} \quad (15)$$

- The bus voltage angle (δ_m) at bus m is constrained by its upper and lower limits ($\delta_m^{\min}$ and $\delta_m^{\max}$) and is determined by equation (16) for all buses.

$$\delta_m^{\min} \le \delta_m \le \delta_m^{\max}, \forall \mathrm{m} \in \{\text{number of buses}\} \quad (16)$$

- The traditional generator's power (p_t) must be limited by its lower and higher limitations ($p_t^{\min}$ and $p_t^{\max}$), which are determined by equation (17).

$$p_t^{\min} \le p_t \le p_t^{\max} \quad (17)$$

- The traditional generator's power (q_t) should be limited by its upper and lower boundaries ($q_t^{\max}$ and $q_t^{\min}$) which are determined by equation (18).

$$q_t^{\min} \le q_t \le q_t^{\max} \quad (18)$$

- Each DG's active power (p_{DG}) is limited by its lower and higher limitations ($p_{DG}^{\min}$ and $p_{DG}^{\max}$) which are determined by equation (19).

$$p_{DG}^{\min} \le p_{DG} \le p_{DG}^{\max} \quad (19)$$

- Each DG's reactive power (q_{DG}) is limited by its lower and upper limitations ($q_{DG}^{\min}$ and $q_{DG}^{\max}$) is calculated using equation (20).

$$q_{DG}^{\min} \le q_{DG} \le q_{DG}^{\max} \quad (20)$$

- Equation (21) states that the overall line loss with DG (p_{DGTLL}) must be less than the overall line loss without DG (p_{TLL}).

$$p_{DGTLL} \le p_{TLL} \quad (21)$$

3. **Performance Indices:** The following is an outline of the system's performance parameters for DG with Ex-PHEV planning:

- **Active Power Loss Index (ILP):** The *ILP* for the impact of DGs with Ex-PHEV is calculated by equation (22).

$$ILP = \frac{\left| p_{WDG} + p_{WEx-PHEV} \right|}{\left| p_{WODG\ \&\ Ex-PHEV} \right|} \times 100 \quad (22)$$

Where $p_{WEx-PHEV}$ denotes the active power loss of DG with Ex-PHEV and $p_{WODG\ \&\ Ex-PHEV}$ denotes the active power loss without DG with Ex-PHEV.

- **Reactive Power Loss Index (ILQ):** The *ILQ* index for the impact of DGs with Ex-PHEV is provided in equation (23).

$$ILQ = \frac{\left|q_{WDG} + q_{WDG\ \&\ Ex-PHEV}\right|}{\left|q_{WODG\ \&\ Ex-PHEV}\right|} \times 100 \tag{23}$$

  Here $q_{WDG\ \&\ Ex-PHEV}$ denotes the reactive power loss of DG with Ex-PHEV and $q_{WODG\ \&\ Ex-PHEV}$ denotes the reactive power loss without a DG with Ex-PHEV.

- **Voltage Deviation Index (IVD):** One advantage of having distinct DG in the proper place and of the appropriate size with Ex-PHEV kinds is the rise in the voltage profile. The index penalizes the $s_{\mathrm{DG}} - l_{DG}$ $s_{Ex-PHEV} - l_{Ex-PHEV}$ pair that offers nominally more varied voltages (V_1 = 1.05 p. u.). As an outcome, the system operates more effectively when the index is close to zero. This has to do with the maximum voltage drop for both the root node and each node. Equation (24) may include the IVD index.

$$\%\,IVD = \max\left(\frac{\left|\overline{V}_1\right| - \left|\overline{V}_i\right|}{\left|\overline{V}_1\right|}\right) \times 100 \text{ for } i = 2 \text{ to } N_B \tag{24}$$

  Here $\overline{V}_1$ denotes the voltage for a slack bus and $\overline{V}_i$ reflects the voltage of DG with Ex-PHEV at the *i*th bus. Because the voltage bounds ($V_{\min} \le V_i \le V_{\max}$) for a specific bus are commonly referred to as technical constraints, the *IVD* value is typically modest and below allowed restrictions.

- **Short circuit capacity index (IC):** With a power source located closer to the load, the power flow might be reduced and some system components could receive more energy. This index is represented by equation (25).

$$\%\,IC = \max\left(\frac{\left|\overline{S}_{ij}\right|}{\left|\overline{CS}_{ij}\right|}\right) \times 100 \quad \text{for } i, j = 1 \text{to } N_L \tag{25}$$

  Here $\overline{CS}_{ij}$ denotes MVA line capacity without DG and $\overline{S}_{ij}$ denotes the MVA line capability for DG with Ex-PHEV.

- **Active power penetration of DGs with Ex-PHEV:** The proportion of the amount of active power for DGs with Ex-PHEV injected within the system and the amount of active power of DG without DG is given by equation (26).

$$\%\,p_{PWDG\&Ex-PHEV} = \frac{p_{WDG} + p_{WEx-PHEV}}{p_{WODG\ \&\ Ex-PHEV} + p_{WDG} + p_{WEx-PHEV}} \times 100 \tag{26}$$

- **Reactive power penetration of DGs with Ex-PHEV:** Equation (27) compares the total reactive power with and without DG to the amount for reactive power from DGs with Ex-PHEV delivered into the system.

$$\%\, p_{QWDG\&Ex-PHEV} = \frac{q_{WDG} + q_{WEx-PHEV}}{q_{WODG\,\&\,Ex-PHEV} + q_{WDG} + q_{WEx-PHEV}} \times 100 \quad (27)$$

III. PROPOSED METHODOLOGY

The several phases for the best placement and size of DGs with Ex-PHEV for ZIP - LMs in GA algorithms, based on the system's minimum total actual power, are listed below:

Step 1: examine the information on the bus system, ZIP - LMs, DGs, and Ex-PHEVs.

Step 2: Run the load flow, or initial fitness solution, for the base case, and compute the indices like (*ILP*, *ILQ*, *IVD*, *IC*, $p_{\text{PWDG \& Ex-PHEV}}$, and $p_{\text{QWDG \& Ex-PHEV}}$) of the base case. Base case record characteristics.

Step 3: The bus system uses binary coding for ZIP - LMs (select one load model at a time), DGs (select one DG at a time), and Ex-PHEV data.

Step 4: Identify the starting the usefulness and fitness of the population: Obtain a random n-chromosome population (a pertinent solution to the issue): arbitrarily obtain $s_{\text{DG}} - l_{DG}$ (select one DG at a time), and $s_{Ex-PHEV} - l_{Ex-PHEV}$ for ZIP - LMs between a predetermined range of $s_{\text{DG}} - l_{DG}$ and $s_{Ex-PHEV} - l_{Ex-PHEV}$.

Step 5: Establish the value of fitness function [f(*x*)] of each $s_{\text{DG}} - l_{DG}$ and $s_{Ex-PHEV} - l_{Ex-PHEV}$ (chromosome) x in the population: run load flow and evaluate indices in the event *ILP*, *ILQ*, *IVD*, *IC*, $p_{\text{PWDG \& Ex-PHEV}}$, and $p_{\text{QWDG \& Ex-PHEV}}$ under a consistent loading scenario for each $s_{\text{DG}} - l_{DG}$ and $s_{Ex-PHEV} - l_{Ex-PHEV}$. Indices and their corresponding $s_{\text{DG}} - l_{DG}$ $s_{Ex-PHEV} - l_{Ex-PHEV}$ pairs are provided in the code itself.

Step 6: Repeat the following processes to create a new population until it is successful:

- Select two parent chromosomes from a population based on fitness (the higher the fitness, the more likely it is that they will be chosen).
- Based on the crossover likelihood, parents switch places to have additional children. When they are no variations, the child and parent are perfect duplicates.
- The mutant probability technique is used to produce new progeny (children) based on every manifestation (chromosome status).
- Using descendants from the most current population.

Verify that restrictions including the voltage deviation limit, the power flow conservation limit, and the thermal ability limit are adhered to. If so, move on to Step 6.

Step 7: Execute the algorithm using the freshly generated population. For every $s_{\mathrm{DG}} - l_{DG}$ and $s_{Ex-PHEV} - l_{Ex-PHEV}$ (chromosomes), test for load flow, and then assess the novel fitness approach. The corresponding indices, like *ILP, ILQ, IVD, IC*, $p_{\mathrm{PWDG\ \&\ Ex\text{-}PHEV}}$, and $p_{\mathrm{QWDG\ \&\ Ex\text{-}PHEV}}$ are further calculated. The attributes of the base case are compared to those of the most recent fitness framework.

Step 8: Stop and select the finest choice from the active options in the present population if any of the stoppage conditions are met.

Step 9: It utilizes the most recent population estimate, including parents and children as a new generation. Does it meet the minimized Multi-Objective function (MOF) condition? Creation of sets k = k + 1 if not. Go to Step 6 now.

A flowchart is shown in Fig. 1 for a suggested strategy called “DGs with Ex-PHEV planning using GA-based multi-objective optimization to minimize system-wide active power loss for ZIP - LMs."

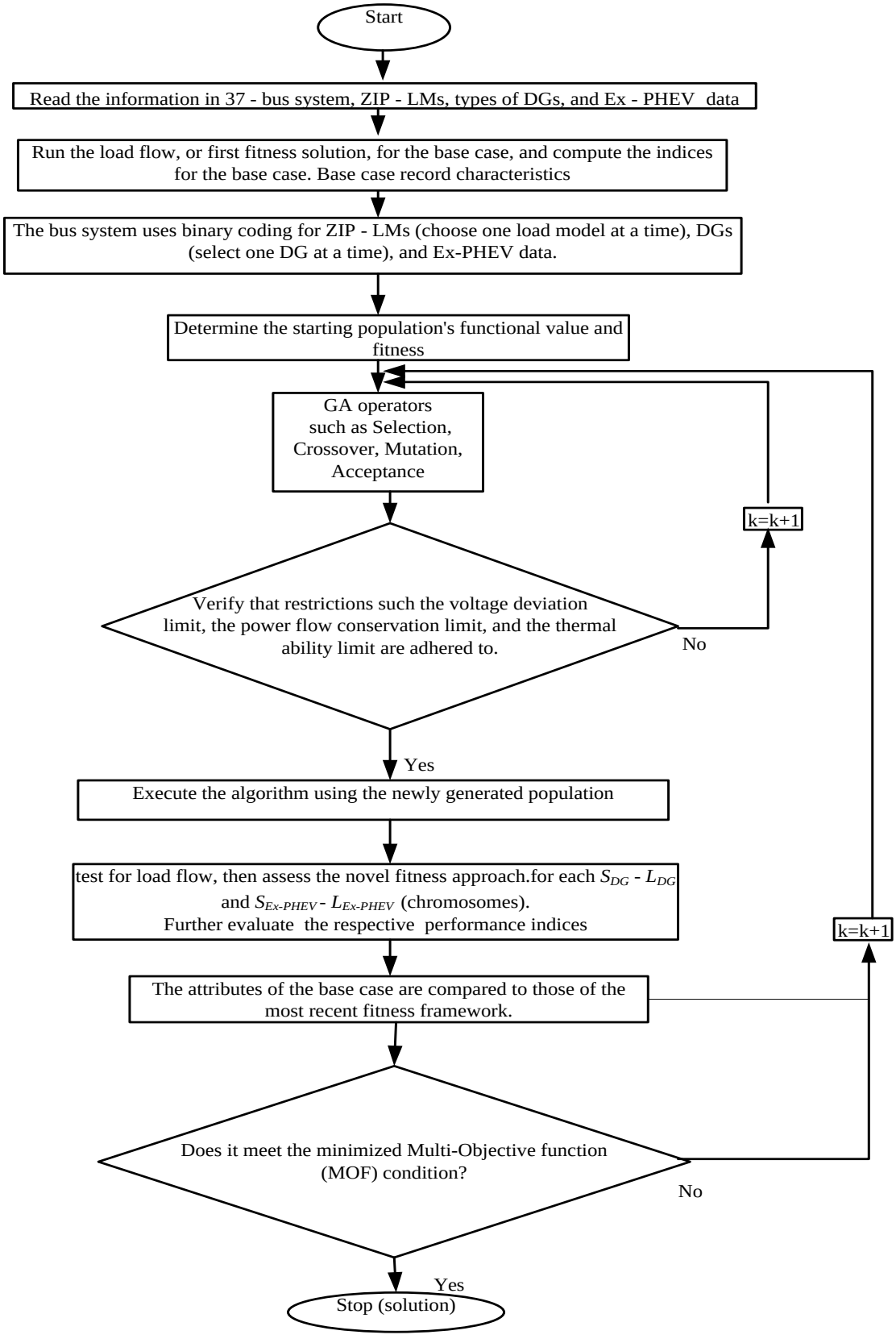

Figure1: Flowchart of GA-based optimization for Impact of DGs with Ex-PHEV in Distribution Systems for ZIP load models.

IV. MULTI-OBJECTIVE FUNCTION-BASED FORMULATIONS

Multi-target simplification difficulties are a frequent occurrence in the design industry. At any level, simplifying the target capabilities at the same time might be advantageous because, by default, they compete with each other and the upgrading procedure necessitates looking for the greatest possible trade approval. Below are the main objectives in the structuring of problems with multi-target progression:

- To ensure unconstrained attention on the target region and associated layout, the selection space is highlighted;
- Begin accumulating algorithmic space in the target environment towards the front Pareto;
- Continue to place a sufficient priority on the Pareto front and optimal Pareto configurations (a good place);
- A predetermined quantity of Pareto based on commitment, for a great enough to give the designer, the manager.

The multi-index for performance evaluation of distribution systems considers all of the preceding indices by providing them critical value in DG rating placement planning to load models. To do so, arrange all effect performance indicators (Values within 0 and 1) in this manner. Specifically concentrating on the MOF that GA has optimized is addressed by equs. (30) - (31).

$$MOF = \varsigma_1\left(ILP\right)+\varsigma_2\left(ILQ\right)+\varsigma_3\left(IVD\right)+\varsigma_4\left(IC\right)+\varsigma_5\left(p_{PWDG\&Ex-PHEV}\right)+\varsigma_6\left(p_{QWDG\&Ex-PHEV}\right) \tag{30}$$

$$\text{Here} \quad \sum_{r=1}^{6}\varsigma_r = 1 \wedge \varsigma_r \in \left(0 \;\; 1\right) \tag{31}$$

Here the values ς_r vary according to their weight in the distribution system's performance indexes. The specific ς_r value is higher if imports from that performance index are preferred over the alternatives. The GA is being used to configure the desired function in the current position. The parity basis listed in Table 1 is used to determine the values of the weights factors. The MOF (specified in (30)) has been reduced back and carries to several functional limitations such as power flow conservation limits, restrictions on short circuit current capacity, and voltage deviation limits [14-15] to satisfy the electrical needs of the distribution system.

V. RESULTS AND DISCUSSIONS

On a 3.0 GHz PC, thorough experimental testing was run using 4096 MB of RAM. The information utilized in the studies relates to a fictitious 37-bus, 12.66 kV system. The base configurations' total substation loads are 2547.32 kVAr and 5084.26 kW. The system is lossy and under-compensated (the total loss is around 8% of the total load). The lossy system is created since it is anticipated that there will be a large loss decrease. For the aforesaid test system's basic values, 100 MVA and 23 kV are used. An informational single-line diagram using the 37-bus system is presented in [15].

Tables 2, 3, 4, and 5 provide an overview of the best outcomes for DGs with Ex-PHEV for ZIP-LMs. Figs. 2, 3, 4, and 5 depict the variations of the real and reactive power loss for ZIP-LMs without and with DGs and Ex-PHEV, respectively. These figures correspond to DGs DG1, DG2, DG3, and DG4.

Concerning other ZIP-LMs, the active power loss minimized (0.0956 p. u.) for the LM5 condition is important. As a result, bus 6 is the best site for DG1. The injection of a single Ex-PHEV into bus no. 26 revealed the LM1-corresponding lowest power loss (0.0540 p. u.). On bus numbers 25 and 4, respectively, double and triple Ex-PHEV injections are made. According to analysis, bus nos. 25 and 4 and LM1 and LM2, respectively, have the lowest power losses (0.0436 p. u. and (0.0322 p. u.) when compared to other ZIP-LMs.

In comparison to previous ZIP-LMs, the power loss minimized (0.0731 p. u.) is significant when DG2 is operating at 0.85 lead power factors for LM5. Therefore, bus 6 is an optimal location for DG2. The injection of a single Ex-PHEV into bus no. 29 revealed the LM4-corresponding lowest power loss (0.0533 p. u.). On bus numbers 6 and 10, respectively, double and triple Ex-PHEV injections are made. The LM2 and bus nos. 6 and 10 are determined to have the lowest power losses (0.0324 p. u.) and (0.0215 p. u.), respectively, when contrasted to other ZIP-LMs.

The power loss minimized (0.1328 p. u.) concerning other ZIP-LMs for the LM5 condition is pertinent. So, bus 31 is the best choice for DG3's location. The injection of a single Ex-PHEV into bus no. 32 revealed the LM3-corresponding lowest power loss (0.1013 p. u.). Similar to this, bus numbers 28 and 29 each receive double and triple Ex-PHEV injections. It was discovered that when compared to ZIP-LMs, LM4, and buses 28 and 29 had the lowest active power losses (0.0863 p. u.) and (0.0658 p. u.), respectively.

In the context of other ZIP-LMs and DG4 operating at 0.85 lag power factor of LM5, the power loss savings (0.1537 p. u.) are significant. Therefore, bus 7 is the best site for DG4 to ride. The injection of a single Ex-PHEV into bus no. 27 revealed the LM5-corresponding lowest power loss (0.0865 p. u.). On buses, no. 28 and 29 double and triple Ex-PHEV are similarly injected. In contrast to other ZIP-LMs, bus nos. 28 and 29 are determined to have the least power loss (0.0585 p. u.) and (0.038 p. u.), respectively.

According to the assessments, bus 6 for DG2 and bus 29 with Ex-PHEV are the best locations in the situations of LM4 because DG2 gives the system real and reactive power at 0.80 to 0.99 leading power factors.

Reactive power loss minimized (0.0682 p. u.) is substantial for other ZIP-LMs under the LM5 condition. As a result, bus 6 is the best site for DG1. The injection of a single Ex-PHEV into bus no. 26 revealed the LM1-corresponding lowest power loss (0.0350 p. u.). On bus numbers 25 and 27, respectively, double and triple Ex-PHEV injections are made. Bus numbers 25 and 27 are determined to have the lowest power losses (0.0212 p. u.) and (0.0109 p. u.), respectively, when compared to other ZIP-LMs.

With DG2 operating at 0.85 lead power factor of LM5 connection in comparison to other ZIP-LMs, the power loss savings (0.0536 p. u.) are significant. Therefore, bus 6 is the optimum location for DG1. The injection of a single Ex-PHEV into bus no. 31 revealed the

LM5-corresponding lowest power loss (0.0324 p. u.). Similar to this, bus numbers 26 and 28 each receive a double and triple injection of Ex-PHEV. When compared to other ZIP-LMs, bus nos. 26 and 28 had the least power loss (0.0256 p. u.) and (0.0197 p. u.), accordingly.

The power loss minimized (0.0901 p. u.) concerning other ZIP-LMs for the LM5 condition is relevant to DG3. So, bus 31 is the best choice for DG3's location. When one Ex-PHEV was injected into bus number 28, the minimum power loss, which corresponds to LM2, was found to be 0.0702 p. u. Similar to this, bus numbers 31 and 28 each receive a double and triple injection of Ex-PHEV. When compared to ZIP-LMs, it was discovered that LM1 and buses no. 31 and 28 had the lowest active power losses (0.0534 p. u.) and (0.0422 p. u.), accordingly.

The power loss minimized (0.1031 p. u.) is pertinent for the LM5 load model condition compared to other ZIP-LMs while DG4 is operating at 0.85 lag power factor. Therefore, bus 7 is the best site for DG4 to ride. The injection of a single Ex-PHEV into bus no. 11 revealed the LM2 to have the smallest power loss (0.0453 p. u.). Similar to this, buses 9 and 10 have double and triple Ex-PHEV injections. In comparison to other ZIP-LMs, bus nos. 9 and 10 had the least power loss (0.0311 p. u.) and (0.0161 p. u.), respectively.

According to the evaluations, bus 6 with DG2 and bus 31 with Ex-PHEV are the best locations in the load condition of the LM5 for minimizing reactive power loss since DG2 gives the system both real and reactive power when the vacuum tube is loaded.

In Figs. 6, 7, 8, and 9, which correspond to DG1, DG2, and DG3, respectively, the variation for the active power loss index and reactive power loss index of DGs with Ex-PHEV for different ZIP-LMs is depicted. It is evident from the profiles that real and reactive power loss patterns are both affected in the same way by DG penetration under ZIP-LM settings.

Figs. 6, 7, 8, and 9 depict the variation for the voltage deviation index of DGs with Ex-PHEV for ZIP-LMs and related to DG1, DG2, DG3, and DG4, accordingly.

The LM5 state is problematic for other ZIP-LMs, and the voltage deviation index decreases (4.8738) are pertinent concerning DG1. As a result, bus 6 is the best site for DG1. The injection of a single Ex-PHEV into bus no. 9 revealed the LM2 to have the smallest power loss (3.3548). On buses no. 7 and 4, respectively, double and triple Ex-PHEV injections are made. According to research, bus numbers 7 and 4 had the least power loss (3.3126) and (3.1872), respectively, when compared to other ZIP-LMs.

The status of LM5 is worrying to other ZIP-LMs, and the voltage deviation index decreases (4.8573) are pertinent with DG2 working at 0.85 lead power factor. As a result, bus 6 is the best site for DG2. The injection of a single Ex-PHEV into bus no. 9 revealed the LM2-corresponding minimum power loss (3.4587). On bus numbers 6 and 10, respectively, double and triple Ex-PHEV injections are made. According to research, bus numbers 6 and 10 had the least power loss (3.4264) and (3.2067), respectively, when compared to other ZIP-LMs.

The state of LM4 is relevant concerning other ZIP-LMs, and the deviation index decreases (6.4379) are pertinent. As a result, bus 7 is the best site for DG3. When one Ex-PHEV was injected into bus number 28, the minimum power loss was found to be (5.2143), which corresponds to LM2. Similar to this, bus numbers 30 and 29 each receive double and triple Ex-PHEV injections. In comparison to ZIP-LMs, it was that which discovered the least active power loss (5.0478) and (4.2646) corresponding to LM3 and LM4 and bus nos. 30 and 29, accordingly.

With DG4 operating at 0.85 lag power factor for the LM2 scenario, the deviation index reductions (7.0262) are pertinent. Therefore, bus 25 is the best place for DG4 to be. The injection of a single Ex-PHEV into bus number 11 revealed the LM2 to have the smallest power loss (4.6874). Similar to this, buses 9 and 10 have double and triple Ex-PHEV injections. According to research, bus nos. 9 and 10 had the least power loss (4.2158) and (4.0236), accordingly, when relative to other ZIP-LMs.

According to the studies of Figs. 6, 7, 8, and 9, bus 7 for DG4 is the optimal place in the LM2 load situation for voltage profile enhancement since DG4 sends active power to the system and either absorbs or supplied reactive power from the systems (based on operating settings).

Figures 6, 7, 8, and 9 depict the distribution for the short circuit line capacity of the DGs and Ex-PHEV for different ZIP-LMs and related to DG1, DG2, DG3, and DG4, accordingly. According to the analysis, the test system is using roughly all of its queue capacity.

Figures 10, and 11, which correspond to DGs 1, 2, and 3 and DG4, respectively, demonstrate the trend of the real and reactive power DG penetration for DGs with Ex-PHEV for different ZIP-LMs. In terms of the active power DG penetration, it is discovered that DG2 exhibits the highest active power DG penetration for ZIP-LMs conditions. In terms of the reactive power DG penetration, the studies show that DG2 exhibits the lowest reactive power DG penetration for ZIP-LMs situations.

VI. RESEARCH CONCLUSIONS AND FUTURE DIRECTIONS

The conclusions and next steps related to the type of work given are then covered in *sub-sections* 1–2

1. **Conclusions:** The following are the analyses of the overall results:-
   - DG2 with Ex-PHEV is shown to have considerable real and reactive power loss limitation in the system under the LM4 condition. Running internal combustion and diesel engines could become economical as a result. At this moment, the system voltage profile has been enhanced as well.
   - It is discovered that various kinds of DGs with Ex-PHEV for ZIP-LMs exhibit unique features for indices including *IPL*, *ILQ*, *IVD*, and *IC*. Lastly, it is emphasized that DG2 offers the system with DG2 real power along with reactive power, improving performance.
   - When DG2 and Ex-PHEV are installed with ZIP - LMs, system performance is enhanced. In addition, the distribution system is utilized to its greatest potential.

- GA-OPF is appropriate in distribution systems for tightly restricted DG and Ex-PHEV assigning issues using ZIP-LMs.

2. **The Future Directions:** The scope of future directions and consequences in this area will include the following suggestion.
   - The application of static computing techniques, along with realistic situations for enhanced performance indices, are also utilized for the appropriately integrated control and ideal positioning of DGs and FACTS controllers.
   - Research on the integration of green energy sources and the development of upcoming power grids is commonly recommended for practitioners to engage in research and also involves the number of success metrics for financial support, improving technological issues, lowering emission levels from the environment, increasing security possibilities and reducing the costs involved.
   - It is recommended that professionals prioritize both renewable resource incorporations and thus the production of expected electricity grids for research works, in addition to providing different performance metrics for appropriately structured various DG regulations and optimal framework placement.
   - The numerous kinds of DGs which are absorbed or supplied into the system used by active and reactive power are classified as a result of the employment of various DG types to meet load demand needs.

VII. LIST OF TABLES AND FIGURES

Table 1: Weight Factors and Their Values on the Parity Basis

Weigh factors	Values on a parity basis
ς_1	0.40
ς_2	0.30
ς_3	0.10
ς_4	0.10
ς_5	0.05
ς_6	0.05

Table 2: dg1 with Ex-PHEV planning for ZIP - LMs

WODG / WDG / Ex-PHEV	ZIP-LMs	S_{DG} (p. u.)	DG PF	DG loc.	Ex-PHEV loc.	p_L (p. u.)	q_L (p. u.)	*% ILP*	*% ILQ*	*% IVD*	*% IC*	% p_{PWDG} & Ex-PHEV	% p_{QWDG} & Ex-PHEV
WODG	-	-	-	-	-	0.1720	0.1145	100	100	7.7070	97.8399	-	-
wdg1	LM1	0.6680	1.00	13	-	0.1232	0.0817	71.3612	71.3612	6.5378	98.0725	45	-
	LM2	2.0351	1.00	6	-	0.0970	0.0689	56.4052	60.1520	5.1010	98.5330	31.29	-
	LM3	2.0753	1.00	6	-	0.0966	0.0686	56.1726	59.9598	5.0515	98.5462	30.79	-
	LM	1.7444	1.00	26	-	0.1008	0.0710	58.6323	61.9867	5.4667	98.4355	34.72	-

	4												
	LM5	2.2186	1.00	6	-	0.0956	0.0682	55.5911	59.5754	4.8738	98.5931	28.96	-
wdg1 + Ex - PHEV (-0.13, -0.0036 p. u.)	LM1	1.5284	1.00	7	26	0.0540	0.0350	50.5678	56.6826	4.3146	100.7036	31	-
	LM2	2.2965	1.00	11	9	0.0653	0.0458	54.2463	58.2187	3.3548	100.9628	25	-
	LM3	2.0652	1.00	5	6	0.0706	0.0554	55.3598	56.2958	3.4258	100.9389	26.2	-
	LM4	2.1028	1.00	28	27	0.0623	0.0619	56.6238	59.7569	4.7589	100.7852	31.8	-
	LM5	2.5364	1.00	6	7	0.0826	0.0478	54.6259	58.4268	3.5236	100.9428	25.8	-
wdg1 + Ex - PHEV	LM1	2.2486	1.00	5	25	0.0436	0.0212	49.7545	53.4365	4.3021	100.7369	28	-
	LM2	2.4997	1.00	26	7	0.0503	0.0322	54.1514	58.1013	3.3126	100.9713	24.8	-
	LM3	1.9556	1.00	10	26	0.0623	0.0411	55.3326	56.2654	3.4125	100.9426	25.8	-

(-0.26,-0.0072 p.u.)	LM4	1.6259	1.00	9	31	0.0447	0.0503	56.6078	59.7265	4.7301	100.8027	30.2	-
	LM5	2.3589	1.00	9	6	0.0628	0.0328	54.5854	57.4127	3.4758	100.9548	25.2	-
wdg1 + Ex-PHEV (-0.39,-0.0108 p.u.)	LM1	2.3327	1.00	8	27	0.0329	0.0109	47.2936	50.1258	4.2103	100.7699	27	-
	LM2	2.5329	1.00	9	4	0.0322	0.0265	54.1077	58.0423	3.1872	100.9816	24.2	-
	LM3	2.2126	1.00	28	9	0.0433	0.0279	55.3069	56.2236	3.3126	100.9533	25.6	-
	LM4	1.6258	1.00	11	13	0.0348	0.0376	56.5835	59.6825	4.7128	100.8923	29.6	-
	LM5	2.4678	1.00	5	8	0.0417	0.0227	51.1053	55.6845	3.4528	100.9824	24.5	-

Table 3: dg2 with Ex-PHEV planning for ZIP - LMs

WODG / WDG / Ex-PHEV	ZIP-LMs	S_{DG} (p. u.)	DG PF	DG loc.	Ex-PHEV loc.	p_L (p. u.)	q_L (p. u.)	% *ILP*	% *ILQ*	% *IVD*	% *IC*	% p_{PWDG} & Ex-PHEV	% p_{QWDG} & Ex-PHEV
WODG	-	-	-	-	-	0.1720	0.1145	100	100	7.7070	97.8399	-	-
wdg2	LM1	0.5545	0.85 ld	31	-	0.1141	0.0758	66.3255	66.2415	6.8311	98.0601	46.46	46.54
	LM2	1.7026	0.85 ld	6	-	0.0779	0.0564	45.2695	49.2486	5.0961	98.4968	37.76	38.04
	LM3	1.7130	0.85 ld	6	-	0.0775	0.0562	45.0602	49.0826	5.0806	98.4998	37.67	37.96
	LM4	1.5103	0.85 ld	27	-	0.0801	0.0582	46.6012	50.8038	5.3854	98.4231	39.39	39.67
	LM5	1.8626	0.85 ld	6	-	0.0731	0.0536	42.4842	46.7849	4.8573	98.5560	36.33	36.67
wdg2 + Ex-PHEV (-0.13, -0.0036 p. u.)	LM1	1.1285	0.85 ld	6	29	0.0648	0.0523	49.6258	50.8256	5.4259	100.8456	42.3	42.1
	LM2	1.4589	0.85 ld	10	9	0.0587	0.0425	42.1257	44.2369	3.4587	100.8689	35.8	35.2
	LM3	1.8561	0.85 ld	13	7	0.0621	0.0462	42.8562	44.6587	3.6321	100.8644	36.1	36.4
	LM4	1.7852	0.85 ld	32	29	0.0533	0.0403	37.2546	39.5326	4.3246	100.7256	35	38.2
	LM5	1.8423	0.85 ld	26	31	0.0546	0.0324	35.3569	38.7852	3.5763	100.8652	37	35.3
	LM1	1.2145	0.85	12	30	0.0482	0.0429	47.5756	49.7869	5.4068	100.8964	35.2	40.4

			ld										
wdg2 + Ex-PHEV (-0.26, -0.0072 p. u.)	LM2	1.6824	0.85 ld	10	6	0.0324	0.0360	41.4862	43.2546	3.4264	100.8965	33.3	33.6
	LM3	1.9582	0.85 ld	7	11	0.0578	0.0365	41.4246	43.2543	3.5205	100.8723	30	34.2
	LM4	1.8542	0.85 ld	26	27	0.0432	0.0326	35.5632	39.4687	3.5423	100.7832	32.8	37
	LM5	1.7568	0.85 ld	24	26	0.0436	0.0256	35.2275	38.7236	3.5125	100.9031	32.1	33
wdg2 + Ex-PHEV (-0.39, -0.0108)	LM1	1.2658	0.85 ld	11	30	0.0269	0.0304	46.0258	47.1146	5.3158	100.8990	32.1	38.6
	LM2	1.9781	0.85 ld	28	10	0.0215	0.0237	39.2586	42.7864	3.2067	100.9864	27	33.1
	LM3	2.1586	0.85 ld	31	7	0.0428	0.0213	40.2579	40.7026	3.4127	100.8950	23.2	32.7
	LM4	2.2367	0.85 ld	8	30	0.0336	0.0220	35.2154	39.0257	3.4576	100.8668	25.2	34.3
	LM5	1.9634	0.85 ld	9	28	0.0325	0.0197	35.2065	38.6321	3.4254	100.9753	21.8	32.2

Table 4: dg3 with Ex-PHEV planning for ZIP - LMs

WODG / WDG / Ex-PHEV	ZIP-LMs	S_{DG} (p. u.)	DG PF	DG loc.	Ex-PHEV loc.	p_L (p. u.)	q_L (p. u.)	*% ILP*	*% ILQ*	*% IVD*	*% IC*	% p_{PWDG} & Ex-PHEV	% p_{QWDG} & Ex-PHEV
WODG	-	-	-	-	-	0.1720	0.1145	100	100	7.7070	97.8399	-	-
	LM1	1.1571	0.00	3	-	0.1589	0.1077	92.7125	94.4634	7.4709	99.9537	-	33.79

wdg3	LM2	1.2579	0.00	6	-	0.1375	0.0930	80.2205	81.6355	6.6572	99.9780	-	31.82
	LM3	1.1405	0.00	31	-	0.1331	0.0905	77.6591	79.4244	6.7806	99.9968	-	34.24
	LM4	1.1835	0.00	7	-	0.1392	0.0947	81.2241	83.1008	6.4379	99.9524	-	33.30
	LM5	1.1071	0.00	31	-	0.1328	0.0901	77.4724	79.0734	6.6804	99.9988	-	34.82
wdg3 + Ex-PHEV (-0.13, -0.0036 p. u.)	LM1	1.2368	0.00	6	29	0.1123	0.0848	75.6584	76.8546	5.5472	99.9645	-	32.2
	LM2	1.5476	0.00	12	28	0.1016	0.0702	74.2543	74.5473	5.2143	99.9913	-	28.2
	LM3	1.2016	0.00	26	32	0.1013	0.0711	73.1258	73.2498	5.2146	99.9985	-	30.1
	LM4	1.6547	0.00	11	27	0.1029	0.0718	78.2567	80.2456	5.2367	99.9733	-	31.6
	LM5	1.0329	0.00	23	30	0.1015	0.0713	74.0264	74.2563	5.3647	99.9993	-	33
wdg3 + Ex-PHEV (-0.26, -0.0072 p. u.)	LM1	1.3654	0.00	30	31	0.0869	0.0534	73.0256	73.5687	5.3481	99.9777	-	31.1
	LM2	1.6421	0.00	8	29	0.0981	0.0633	73.1242	73.3215	5.2048	99.9980	-	27.3
	LM3	1.2252	0.00	7	30	0.0937	0.0688	70.1023	73.2546	5.0478	99.9993	-	29.6
	LM4	1.3325	0.00	11	28	0.0863	0.0628	75.1257	74.5476	5.2047	99.9917	-	28
	LM5	1.1256	0.00	5	31	0.0944	0.0602	72.0257	73.2486	5.2149	99.9996	-	32.1
wdg3 + Ex-PHEV (-0.39, -0.0108)	LM1	1.3249	0.00	32	28	0.0664	0.0422	71.1254	72.5469	5.5789	99.9827	-	30
	LM2	1.2357	0.00	7	32	0.0861	0.0512	71.0215	72.2546	5.1259	99.9991	-	23.1
	LM3	2.3624	0.00	8	28	0.0788	0.0538	66.1258	73.1573	4.6547	99.9997	-	28.5
	LM4	1.5321	0.00	31	29	0.0658	0.0524	72.2547	72.12547	4.2646	99.9981	-	27.9
	LM5	1.3245	0.00	10	27	0.0749	0.0460	70.2547	72.2486	5.1268	99.9998	-	30.4

Table 5: dg4 with Ex-PHEV planning for ZIP - LMs

WODG / WDG / Ex-PHEV	ZIP-LMs	S_{DG} (p. u.)	DG PF	DG loc.	Ex-PHEV loc.	p_L (p. u.)	q_L (p. u.)	*% ILP*	*% ILQ*	*% IVD*	*% IC*	% p_{PWDG} & Ex-PHEV	% p_{QWDG} & Ex-PHEV
WODG	-	-	-	-	-	0.1720	0.1145	100	100	7.7070	97.8399	-	-
wdg4	LM1	1.0479	0.85 lg	7	-	0.1541	0.1032	89.6261	90.1188	7.1214	98.0473	43.26	55.20
	LM2	1.2264	0.85 lg	25	-	0.1544	0.1041	89.8064	90.9051	7.0262	98.0819	41.96	55.12
	LM3	1.2121	0.85 lg	3	-	0.1539	0.1040	89.7598	90.8352	7.0340	98.0784	42.06	55.29
	LM4	1.0952	0.85 lg	27	-	0.1540	0.1033	89.6319	90.2761	7.0961	98.0567	42.92	55.41
	LM5	1.0594	0.85 lg	7	-	0.1537	0.1031	89.6145	90.1450	7.1155	98.0495	43.18	55.26
wdg4 + Ex-PHEV (-0.13, -0.0036 p. u.)	LM1	1.1628	0.85 lg	24	6	0.1036	0.0788	69.5879	78.2254	5.5248	100.3698	42.7	42.1
	LM2	1.3246	0.85 lg	32	11	0.0936	0.0453	58.2549	57.5496	4.6874	100.4580	38.2	41.1
	LM3	1.2546	0.85 lg	14	7	0.0925	0.0810	55.0259	61.7562	5.1207	100.3502	40.8	39.4
	LM4	1.9963	0.85 lg	24	25	0.1036	0.0769	74.5472	72.6574	5.5872	100.1256	34.1	34.3
	LM5	1.3248	0.85 lg	7	27	0.0865	0.0613	59.1256	62.2358	5.4586	100.3548	42.5	40.1
	LM1	1.7548	0.85 lg	8	7	0.0823	0.0603	58.2568	61.2249	4.7852	100.5258	41.3	40.3

wdg4 + Ex-PHEV (-0.26, -0.0072 p. u.)	LM2	1.2358	0.85 lg	6	9	0.0801	0.0311	55.65842	56.1259	4.2158	100.5125	39.2	39.6
	LM3	1.2540	0.85 lg	34	8	0.0729	0.0521	53.1257	53.5284	4.5157	100.4025	39.1	36.4
	LM4	1.3648	0.85 lg	17	27	0.089	0.0528	56.6587	60.5879	5.0258	100.3789	33.8	32.1
	LM5	1.2355	0.85 lg	10	28	0.0585	0.0458	54.1253	55.5486	4.5486	100.4125	41.8	38.6
wdg4 + Ex-PHEV (-0.39, -0.0108)	LM1	1.7568	0.85 lg	9	8	0.056	0.0428	55.4581	54.5782	4.2548	100.6238	40	38.6
	LM2	1.1257	0.85 lg	6	10	0.0632	0.0161	54.2579	54.6547	4.0236	100.7985	36.4	36.8
	LM3	1.4539	0.85 lg	24	9	0.0458	0.0364	47.8761	49.2587	4.3684	100.4958	36.2	31.8
	LM4	1.3548	0.85 lg	10	28	0.0721	0.0325	53.8548	55.4582	4.5423	100.4358	32.7	27.1
	LM5	1.3245	0.85 lg	7	29	0.038	0.0236	52.1256	53.5486	4.1025	100.5201	40.6	34.3

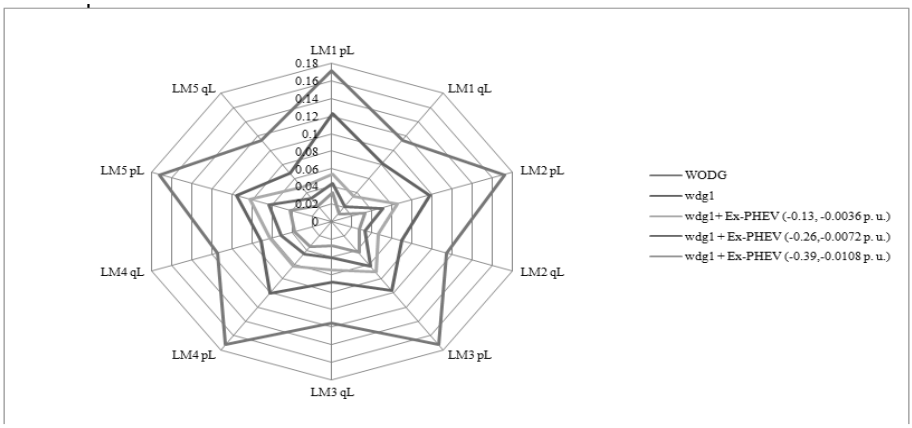

Figure 2: Profile assessment for p_L (p. u.) and q_L (p. u.) of dg1 with Ex-PHEV

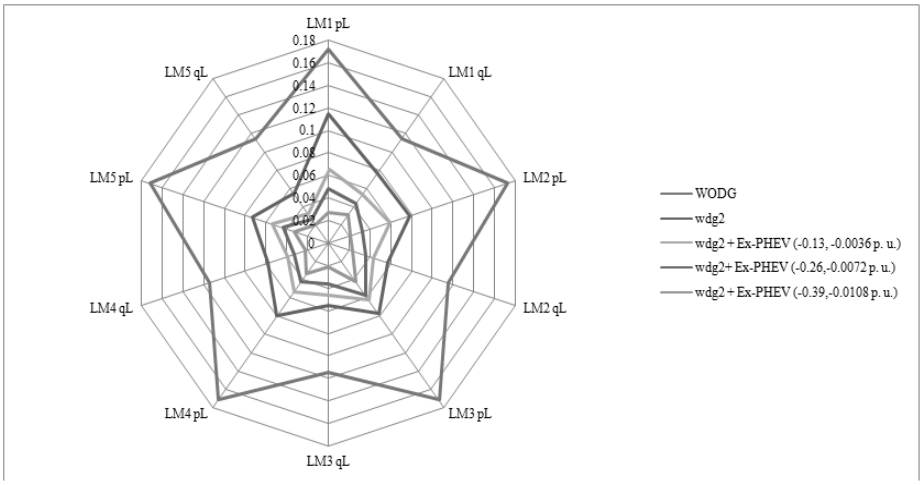

Figure 3: Profile Assessment for p_L (p. u.) and q_L (p. u.) of dg2 with Ex-PHEV

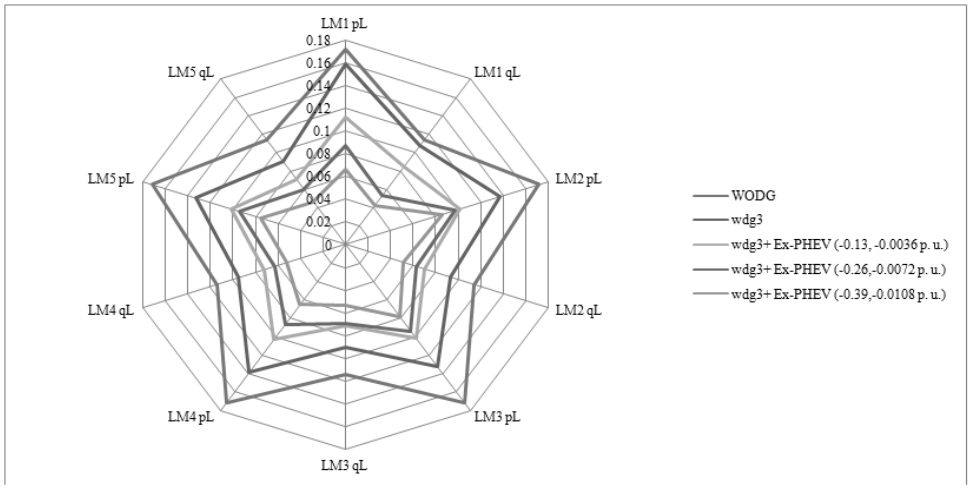

Figure 4: Profile Assessment for p_L (p. u.) and q_L (p. u.) of dg3 with Ex-PHEV

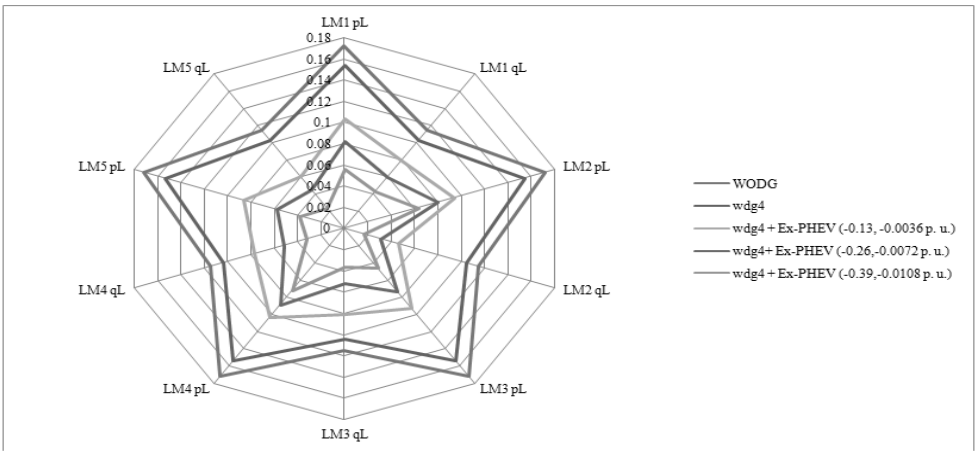

Figure 5: Profile Assessment for p_L (p. u.) and q_L (p. u.) of dg4 with Ex-PHEV

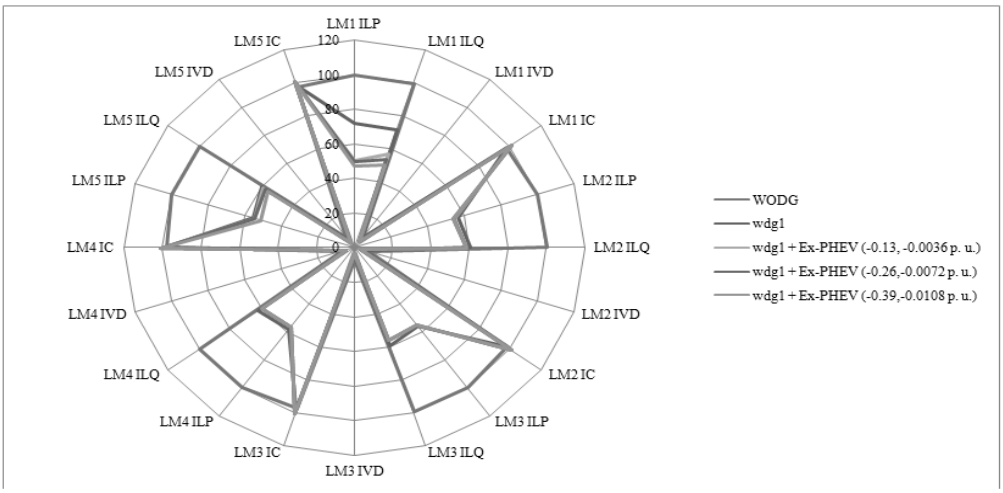

Figure 6: Profile Assessment of % *ILP*, % *ILQ*, % *IVD*, and % *IC* for dg1 with Ex-PHEV

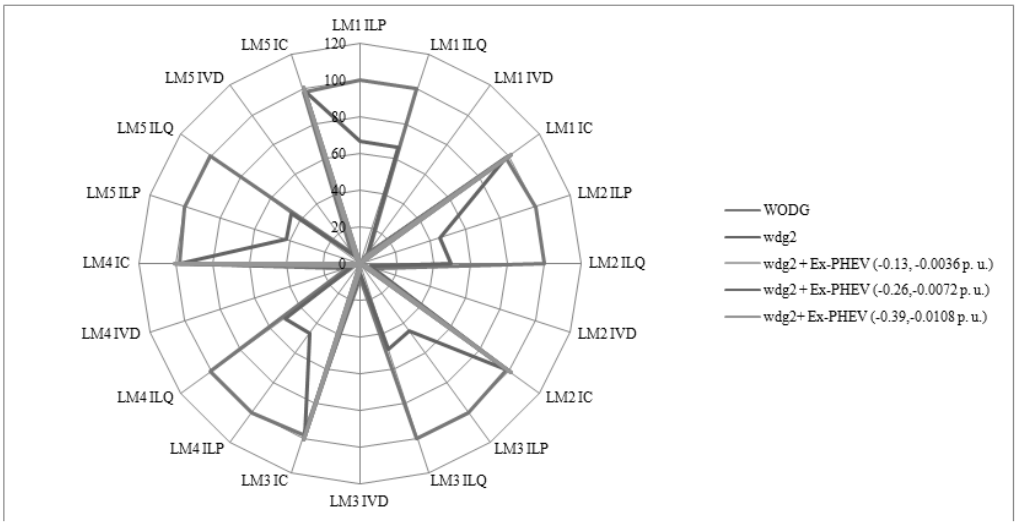

Figure 7: Profile Assessment of % *ILP*, % *ILQ*, % *IVD*, and % *IC* for dg2 with Ex-PHEV

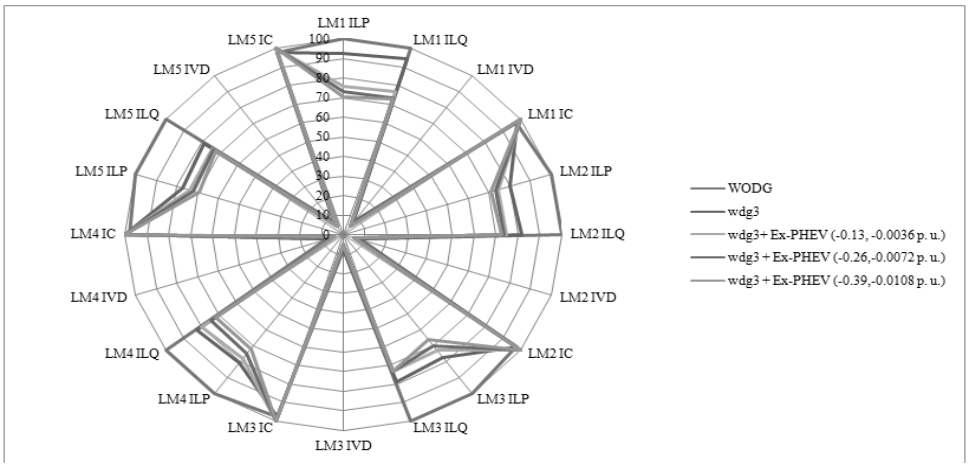

Figure 8: Profile Assessment of % *ILP*, % *ILQ*, % *IVD*, and % *IC* for dg3 with Ex-PHEV

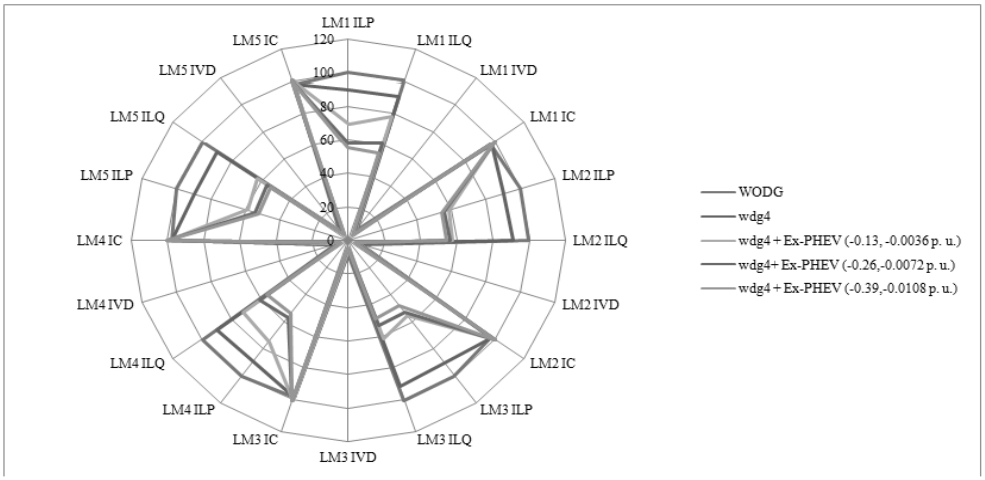

Figure 9: Profile Assessment of % *ILP*, % *ILQ*, % *IVD*, and % *IC* for dg4 with Ex-PHEV

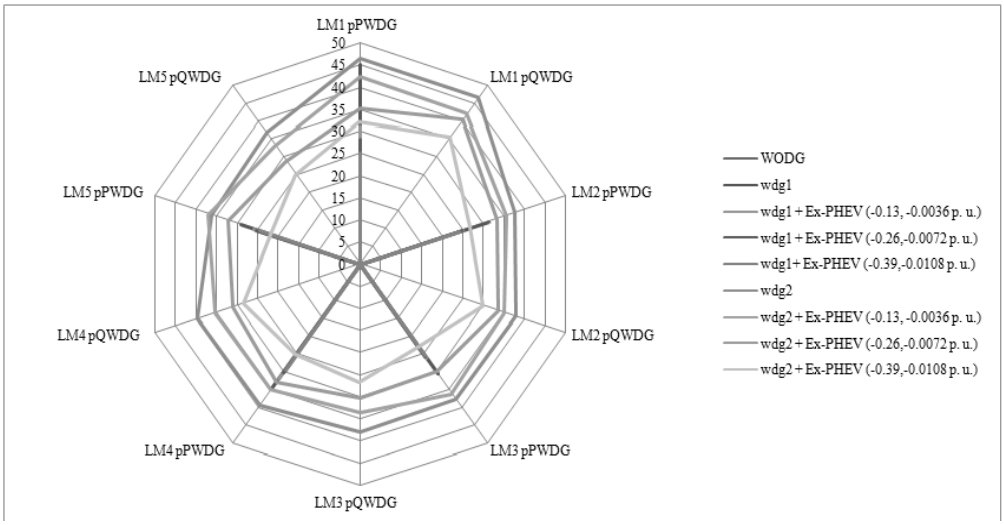

Figure 10: Profile Assessment of % $p_{PWDG\ \&\ Ex\text{-}PHEV}$ and % $p_{QWDG\ \&\ Ex\text{-}PHEV}$ for dg1

with Ex-PHEV and dg2 with Ex-PHEV

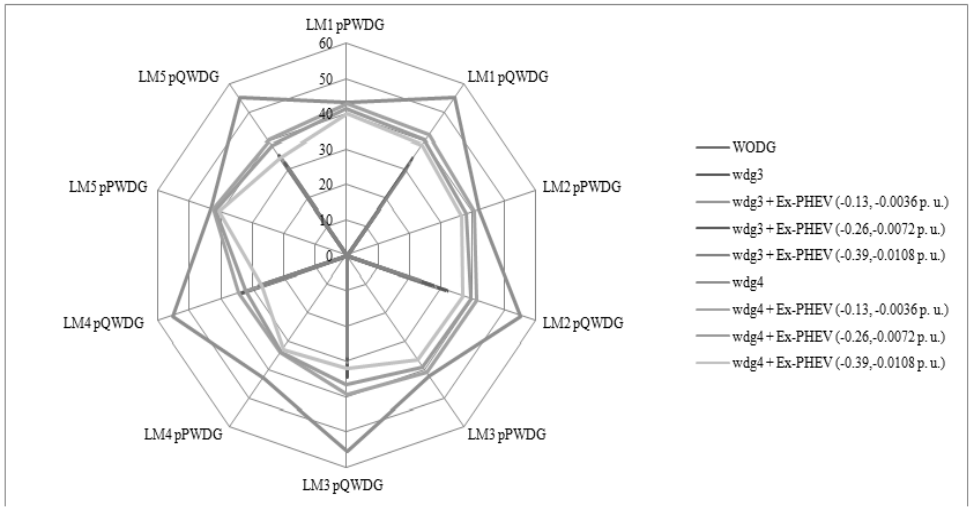

Figure 11: Profile Assessment of % $p_{PWDG\ \&\ Ex\text{-}PHEV}$ and % $p_{QWDG\ \&\ Ex\text{-}PHEV}$ for dg3 with Ex-PHEV and dg4 with Ex-PHEV

REFERENCES

[1] Galiveeti, Hemakumar Reddy, Arup Kumar Goswami, and Nalin B.Dev Choudhury, "Impact of plug-in electric vehicles and distributed generation on reliability of distribution systems" Engineering Science and Technology, an International Journal vol. 21, no. 1, 2018, pp. 50 - 59.

[2] S. Pazouki, A. Mohsenzadeh, S. Ardalan, and M. Haghifam, "Simultaneous Planning of PEV Charging Stations and DGs Considering Financial, Technical, and Environmental Effects," Canadian Journal of Electrical and Computer Engineering, vol. 38, no. 3, pp. 238-245, 2015.

[3] S. J. Gunter, K. K. Afridi, and D. J. Perreault, "Optimal Design of Grid-Connected PEV Charging Systems With Integrated Distributed Resources," IEEE Trans. Smart Grid, vol. 4, no. 2, pp. 956 - 967, 2013.

[4] S. F. Abdelsamad, W. G. Morsi and T. S. Sidhu, "Impact of Wind-Based Distributed Generation on Electric Energy in Distribution Systems Embedded With Electric Vehicles," IEEE Trans. Sustainable Energy, vol. 6, no. 1, pp. 79 - 87, 2015.

[5] U. C. Chukwu and S. M. Mahajan, "V2G Parking Lot with PV Rooftop for Capacity Enhancement of a Distribution System," IEEE Trans. Sustainable Energy, vol. 5, no. 1, pp. 119 - 127, 2014.

[6] S. Gao, K. T. Chau, C. Liu, D. Wu, and C. C. Chan, "Integrated Energy Management of Plug-in Electric Vehicles in Power Grid With Renewable," IEEE Trans. Vehicular Technology, vol. 63, no. 7, pp. 3019 - 3027, 2014.

[7] J. Zhao, Z. Xu, J. Wang, C. Wang, and J. Li, "Robust Distributed Generation Investment Accommodating Electric Vehicle Charging in a Distribution Network," IEEE Trans. Power Systems, vol. 33, no. 5, pp. 465 - 4666, 2018.

[8] Z. Fan et al., "Multi-Objective Planning of DGs Considering ES and EV Based on Source-Load Spatiotemporal Scenarios," IEEE Access, vol. 8, pp. 216835 - 216843, 2020.

[9] A. Ahmadian, M. Sedghi, and M. Aliakbar-Golkar, "Fuzzy Load Modeling of Plug-in Electric Vehicles for Optimal Storage and DG Planning in Active Distribution Network," IEEE Trans. Vehicular Technology, vol. 66, no. 5, pp. 3622 - 3631, 2017.

[10] H. Zhang, S. J. Moura, Z. Hu, W. Qi, and Y. Song, "Joint PEV Charging Network and Distributed PV Generation Planning Based on Accelerated Generalized Benders Decomposition," IEEE Trans. Transportation Electrification, vol. 4, no. 3, pp. 789 - 803, 2018.

[11] Z. Liu, Q. Wu, M. Shahidehpour, C. Li, S. Huang, and W. Wei, "Transactive Real-Time Electric Vehicle Charging Management for Commercial Buildings With PV On-Site Generation," IEEE Trans. Smart Grid, vol. 10, no. 5, pp. 4939 - 4950, 2019.

[12] S. Wang, Z. Y. Dong, C. Chen, H. Fan, and F. Luo, "Expansion Planning of Active Distribution Networks With Multiple Distributed Energy Resources and EV Sharing System," IEEE Trans. Smart Grid, vol. 11, no. 1, pp. 602 - 611, 2020.
[13] S. Ganguly and D. Samajpati, "Distributed Generation Allocation on Radial Distribution Networks Under Uncertainties of Load and Generation Using Genetic Algorithm," IEEE Trans. Sustainable Energy, vol. 6, no. 3, pp. 688 - 697, 2015.
[14] Singh D, Mishra RK, Singh D. Effect of load models on distributed generation planning. IEEE Trans. Power Syst., vol. 22, no. 4, pp. 2204 – 12, 2007.
[15] Singh D, Singh D, Verma KS. Multi-objective optimization for DG planning with load models. IEEE Trans. Power Syst., vol. 24, no. 1, pp. 427 – 36, 2009.
[16] Bokhari A, Alkan A, Dogan R, Aguilo MD, Leon F, Czarkowski D, Zabar Z, Birenbaum L, Noel A, Uosef RE. Experimental Determination of the ZIP Coefficients for Modern Residential, Commercial, and Industrial Loads. IEEE Trans. Power Delivery; vol. 29, no. 3, pp. 1372-1381, 2014
[17] A. Arif, Z. Wang, J. Wang, B. Mather, H. Bashualdo and D. Zhao, "Load Modeling—A Review," in IEEE Transactions on Smart Grid, vol. 9, no. 6, pp. 5986 - 5999, 2018.
[18] Patel, D. K., Singh, D., & Singh, B. Genetic algorithm- based multi- objective optimization for distributed generations planning in distribution systems with constant impedance, constant current, constant power load models. International Transactions on Electrical Energy Systems, vol. 30, no. 11, 2020.
[19] X. Tang, T. Jia, X. Hu, Y. Huang, Z. Deng, and H. Pu, "Naturalistic Data-Driven Predictive Energy Management for Plug-In Hybrid Electric Vehicles," IEEE Trans. Transportation Electrification, vol. 7, no. 2, pp. 497-508, 2021.
[20] X. Hu, C. Zou, X. Tang, T. Liu, and L. Hu, "Cost-Optimal Energy Management of Hybrid Electric Vehicles Using Fuel Cell/Battery Health-Aware Predictive Control," IEEE Trans. Power Electronics, vol. 35, no. 1, pp. 382-392, 2020.
[21] Dilip Kumar Patel, Deependra Singh, Bindeshwar Singh, A comparative analysis for impact of distributed generations with electric vehicles planning, Sustainable Energy Technologies and Assessments, Volume 52, Part A, 2022, 101840, ISSN 2213-1388, https://doi.org/10.1016/j.seta.2021.101840.

